

Supplemental Materials

Molecular Biology of the Cell

Wueseke et al.

Figure S1 – SPD-2 and SPD-5::GFP co-immunoprecipitate from centrosome containing extracts.

Western blot analysis showing SPD-5::GFP and SPD-2 co-immunoprecipitation using GFP targeted immuno precipitation from centrosome containing low spin extract and cytoplasmic high spin extract. Cytoplasmic extracts were prepared as described in this paper, centrosome containing extracts were prepared as described by (Mitchison and Kirschner, 1984; Bornens *et al.*, 1987). Briefly, after sonication centrosome containing extracts were spun at 1,200 xg for 10 minutes and the supernatant was directly used for immuno precipitation. His targeting beads were used to control for unspecific binding.

Figure S2 – Supporting information for fluorescence correlation spectroscopy experiments depicted in Figure 3

(A) Immuno blots showing the successful run down of RSA-2, SPD-2 and PLK-1 after 24 hrs of respective RNAi. Full depletion was achieved after 24 hrs for all proteins. Note that the feeding clone used here to knock down SPD-2 is not the *spd-2-rr* clone used for the embryo viability assay, for more information see Material and Methods. (B) Top box: Exemplary fit of a normalized autocorrelation curve (black line) from a single embryo. Red line indicates the fit, the red vertical line the position of the calculated characteristic diffusion time τ , green vertical lines indicate the fit boundaries. Diffusion time (D) and reduced Chi square (χ_r^2) as calculated from the fit are given for this particular fit. Bottom box: Residual trace showing the deviations of the raw data from the fit. (C) R^2 -values and χ_r^2 -values, indicating the fit quality for the fits of all GFP::SPD-2 FCS measurements. (D) R^2 -values and χ_r^2 -values, indicating the fit quality for the fits of all LAP::RSA-1 FCS measurements.

Figure S3 – The mobility of SPD-5 is unaffected by RSA-2 depletion

(A) Autocorrelation curves measured in SPD-5::GFP embryos under wild type and *rsa-2* RNAi conditions. (B) Diffusion coefficients obtained from the fits of the autocorrelation curves for SPD-5::GFP. Diffusion under wild type

conditions was $1.4 \pm 0.2 \mu\text{m}^2/\text{s}$ ($n = 14$), and $1.4 \pm 0.2 \mu\text{m}^2/\text{s}$ under *rsa-2* RNAi ($n = 17$). (C) Antibody-guided depletion of RSA-2 from extracts did not affect the hydrodynamic radius of SPD-5. Immuno blot analysis of the size exclusion chromatography fractionation of showing SPD-5, RSA-2 and RSA-1 immuno blots. RSA-2 was almost fully depleted, and with it the majority of RSA-1. Fractions were collected in 0.5 ml steps. The peak fraction of SPD-5 is indicated by black arrowhead. The hydrodynamic radius of SPD-5 was calculated to be 9.4 nm. Peak fractions of standard proteins are drawn as black arrowheads with the according hydrodynamic radius above the top lane. (D) Antibody-guided depletion of RSA-2 from extracts did not affect the Svedberg coefficient of SPD-5. An immunoblot of the 25 x 0.2 ml fractions obtained from a 5 ml 15-55 % sucrose gradient used in rate zonal ultracentrifugation is shown. The peak fraction of SPD-5 is indicated by black arrowhead. The Svedberg coefficient was found to be 3.7 S. The centers of the peaks for each standard protein are indicated along with their Svedberg coefficients by the black arrowheads above the top lane.

Figure S4 – AIR-1 depletion does not affect SPD-5::GFP or GFP::SPD-2 diffusion.

(A) Western blot showing successful reduction of AIR-1 levels to about 8% of initial levels after 32 hrs of *air-1* RNAi. (B) Autocorrelation curves from SPD-5::GFP measurements in wild type and AIR-1 depleted embryos. (C) Diffusion coefficients obtained from fitting autocorrelation curves from SPD-5::GFP measurements, diffusion of SPD-5::GFP under wild type conditions was $1.3 \pm 0.3 \mu\text{m}^2/\text{s}$ and $1.2 \pm 0.3 \mu\text{m}^2/\text{s}$ under *air-1* RNAi. (D) Autocorrelation curves from GFP::SPD-2 measurements in wild type and AIR-1 depleted embryos. (E) Diffusion coefficients obtained from fitting autocorrelation curves from SPD-5::GFP measurements, diffusion of GFP::SPD-2 under wild type conditions was $2.7 \pm 0.8 \mu\text{m}^2/\text{s}$ and $2.6 \pm 0.9 \mu\text{m}^2/\text{s}$ under *air-1* RNAi.

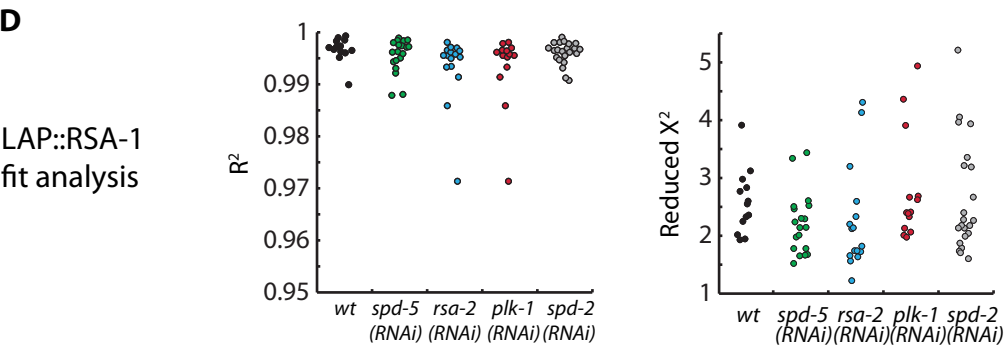
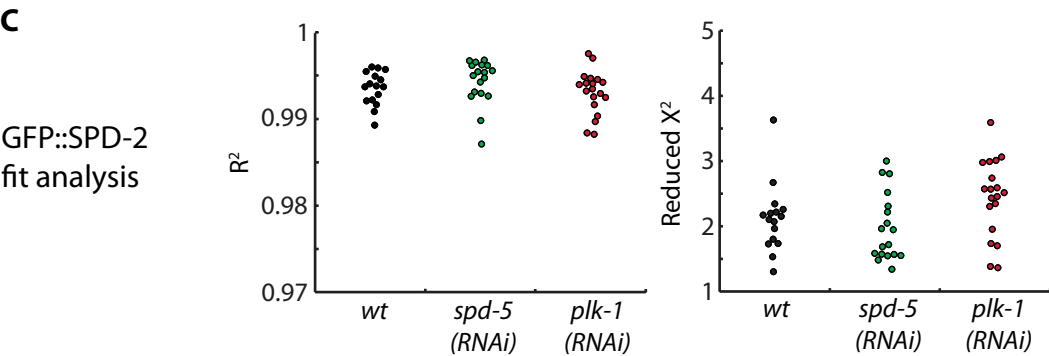
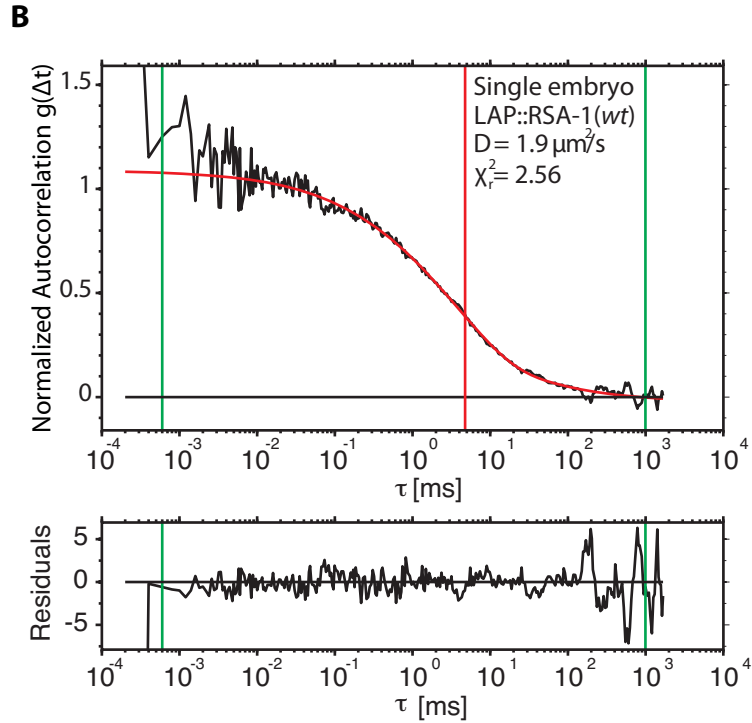
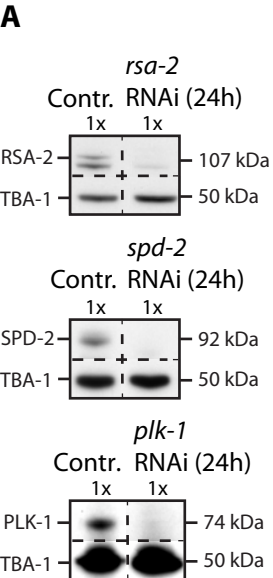
Figure S5 – Information on Mos1 integration of *spd-2* transgene

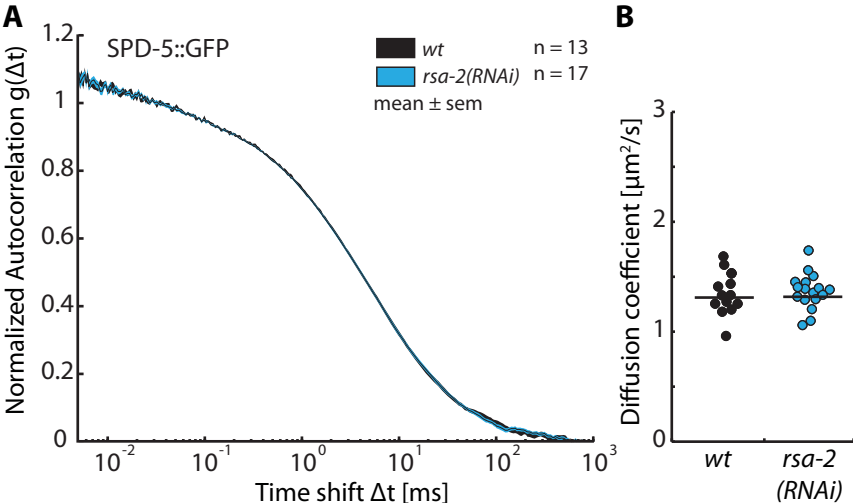
Schematic of the Mos1 integration strategy used to generate single copy transgenic lines expressing GFP::SPD-2. Shown below is an overview of specific sequences of interest used in the generation of the constructs.

References:

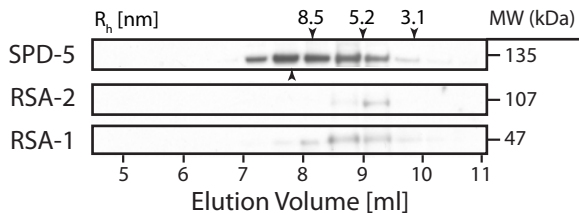
Bornens, M., Paintrand, M., Berges, J., Marty, M. C., and Karsenti, E. (1987). Structural and chemical characterization of isolated centrosomes. *Cell Motil Cytoskeleton* 8, 238–249.

Mitchison, T., and Kirschner, M. (1984). Microtubule assembly nucleated by isolated centrosomes. *Nature* 312, 232–237.

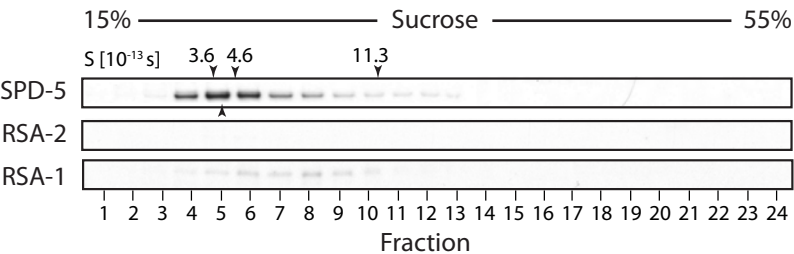


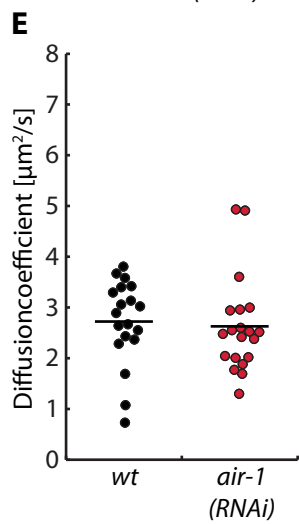
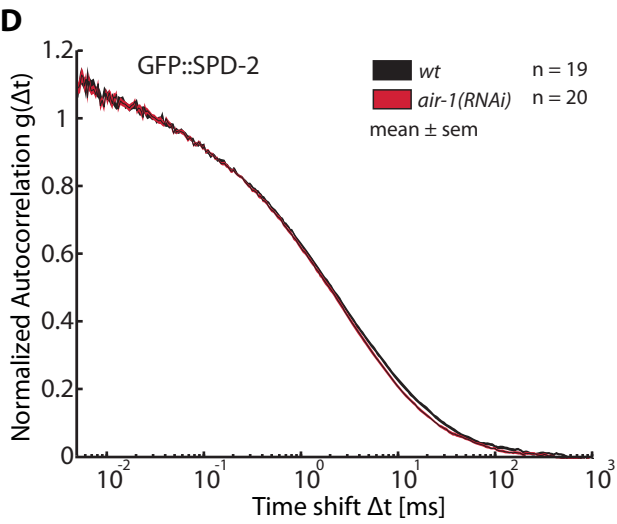
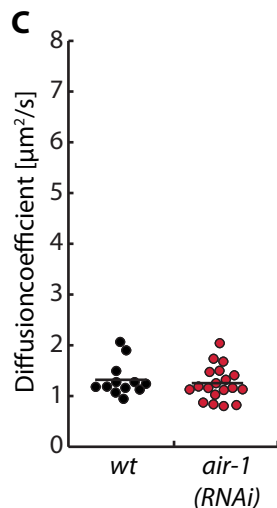
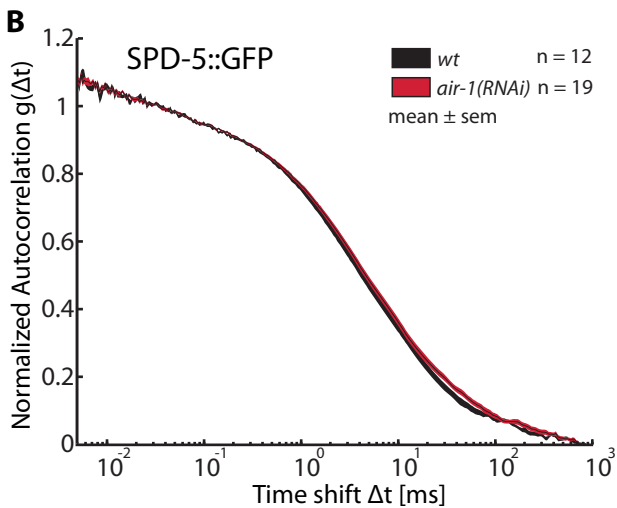
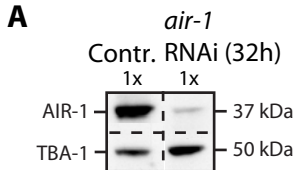


C Size exclusion chromatography of RSA-2 depleted extracts



D Rate zonal ultracentrifugation of RSA-2 depleted extracts





Single copy RNAi-resistant transgene
insertion encoding **GFP::SPD-2**

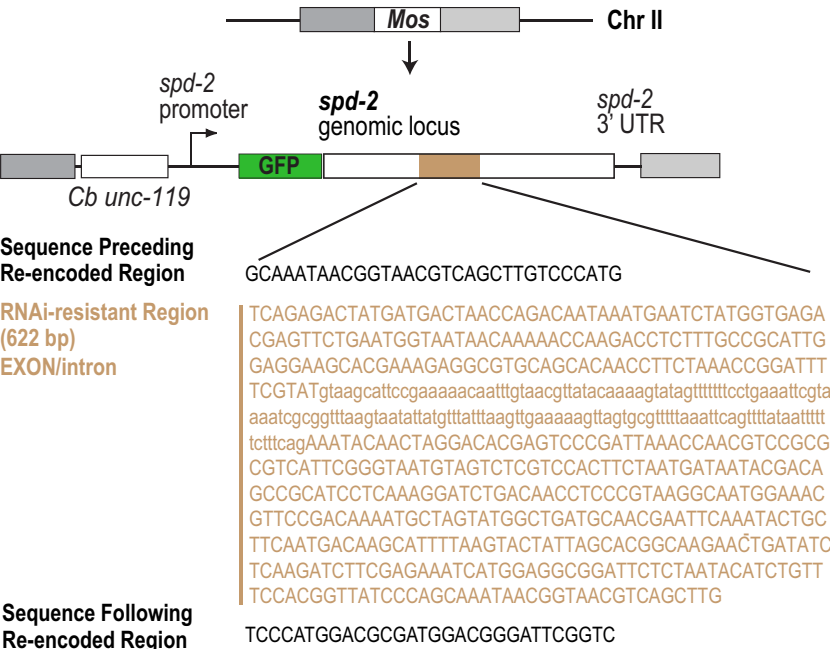


Table S1 - *C. elegans* strains used in this study

Strain no.	Genotype	Reference
N2	wild type (ancestral)	(Brenner, 1974)
TH27	<i>unc-119(ed3) III; ddIs6 [GFP:: tbg-1; unc-119(+)]</i>	(Hannak <i>et al.</i> , 2001)
TH105	<i>unc-119(ed3)III; ddIs14 [pie-1::LAP::rsa-1; unc-119(+)]</i>	(Schlitz <i>et al.</i> , 2007)
TH327	<i>unc-119(ed3)III; ddIs64 [pie-1::SPD-5(synthetic introns, CAI 0.65)::GFP; unc-119(+)]</i>	(Decker <i>et al.</i> , 2011)
OD824	<i>ItSi203[pVV60; Pspd-2::GFP::SPD-2 reencoded; cb-unc-119(+)]II; unc-119(ed3) III</i>	
EG4322	<i>ttTi5605 II; unc-119(ed9) III.</i>	(Frøkjær-Jensen <i>et al.</i> , 2008)